

Calibration of Lead-Line Response Contribution in Measured Radiation Patterns of IR Dipole Arrays

Peter M. Krenz, *Student Member, IEEE*, Brian A. Lail, and Glenn D. Boreman

Abstract—A bolometer, which is in the shape of an antenna, is investigated as an infrared detector. Similar to antenna-coupled bolometers, this device can be designed to meet specific spectral, polarization, and directional criteria. The fabricated device is not an isolated antenna; it contains lead lines for biasing and signal extraction, which also respond to the incident radiation and contribute to the measured response. An additional device is designed to measure this response component, which is then removed from the measured response of the device containing the antenna. The measured radiation patterns without lead-line contributions show excellent agreement with the simulated patterns.

Index Terms—Bolometric antenna, infrared antenna, numerical simulation, radiation pattern.

I. INTRODUCTION

THE ANTENNA portion of infrared (IR) antenna-coupled bolometers modifies the spectral, polarization, and directional sensitivity of the bolometer [1]. To facilitate a straightforward and rapid fabrication process in this paper, the antenna is not coupled to a bolometer [2], but instead, the bolometer is shaped to form an antenna. The response is not measured by a discrete sensor element at the feedpoint of the antenna, but since the entire device is composed of gold, which has a temperature coefficient of resistance (TCR) of 0.37%/K at room temperature [3], all sections of the antenna will contribute to the measured response.

The spectral, polarization, and directional properties of the distributed bolometer antenna can be designed similar to an antenna-coupled bolometer. The bolometric antenna is composed of a material that is more lossy compared to the metal that is used for an antenna-coupled bolometer. The electromagnetic energy is dissipated in the entire structure due to this loss and causes the change in temperature of the bolometric antenna, which is measured. An antenna composed of material with higher loss will have modified spectral properties when compared to an ideal antenna. The resonance is damped and broadened, as well as shifted toward lower frequencies [4]. The higher loss of the antenna also impacts the directional properties of the detector. The directivity is reduced and the width of the main beam is increased [5]. The polarization-sensitive response

of the antenna is related to its geometry rather than its material properties and is therefore not affected by an increase of loss in the antenna material.

The investigated receiving antennas are one-, two-, three-, and four-dipole arrays that are separated from a ground plane by a dielectric standoff layer. The biasing and readout circuits also respond to the incident radiation. With an interest in the primary antenna-array response and due to limitations in the computational resources and time required to simulate the entire structure, including the lead lines, we model the antenna array without lead lines. The lead-line response contribution is measured by a reference device and subtracted from the distributed-antenna response. Excellent agreement between the measured and simulated radiation pattern without lead-line response contributions is demonstrated, indicating that the presented simulation technique can be used to optimize a distributed-antenna design.

II. BOLOMETER SIMULATION IN HFSS

Ansoft high-frequency structure simulator (HFSS) is used to simulate the antenna arrays, which are designed to operate at the main CO₂ laser line of 28.3 THz. To ensure a successful fabrication process, several dimensions of the device layout are fixed before optimizing the dipole length and element separation using the simulation software. The gold dipoles are 200 nm wide and 75 nm thick and the dielectric standoff layer, which is cyclotene (BCB) [6], is 1.6 μm thick. A J. A. Woollam IR variable-angle spectroscopic ellipsometer (IR-VASE) [7] was used to measure the at-frequency relative permittivity of gold ($\epsilon'_r = -4787$ and $\epsilon''_r = 1630$) and BCB ($\epsilon'_r = 2.36$ and $\epsilon''_r = 0.071$) films of the appropriate thicknesses. In the simulation, these properties are assigned to the antenna and standoff layer. The bottom boundary of the dielectric layer is the ground plane, which is simulated as a perfect electric conductor. All other boundaries of the volume enclosing the antenna and standoff layer are terminated with PMLs. This termination will absorb any radiation traveling toward it without causing back reflections, essentially simulating that the dielectric standoff layer has an infinite extent along the plane of the air–dielectric boundary.

The antenna is illuminated by a plane wave that is polarized parallel to the axis of the dipole, and the electric field and current density are computed inside the gold structure. The bolometric response is proportional to the power dissipated in the bolometer volume, which is, in this case, the entire antenna, due to ohmic loss [8]. Computations using the simulated-field quantities can be performed with the HFSS “fields-calculator” feature. The ohmic loss is computed by integrating the dot product of the electric field and complex conjugate of the current density over

Manuscript received January 28, 2010; revised March 15, 2010; accepted March 16, 2010. Date of publication April 29, 2010; date of current version February 4, 2011.

P. M. Krenz and G. D. Boreman are with the College of Optics and Photonics (CREOL), University of Central Florida, Orlando, FL 32816 USA (e-mail: pkrenz@creol.ucf.edu; boreman@creol.ucf.edu).

B. A. Lail is with the Electrical and Computer Engineering Department, Florida Institute of Technology, Melbourne, FL 32901 USA (e-mail: blail@fit.edu).

Color versions of one or more of the figures in this paper are available online at <http://ieeexplore.ieee.org>.

Digital Object Identifier 10.1109/JSTQE.2010.2046398

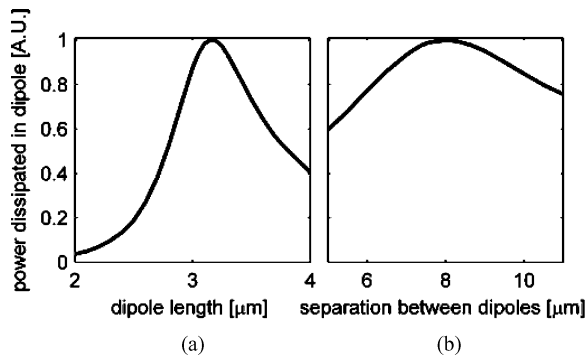


Fig. 1. Optimal dipole length is found by computing the power dissipated while varying the dipole length. (a) Largest response is expected at $3.2 \mu\text{m}$. (b) Two $3.2\text{-}\mu\text{m}$ -long dipoles with varying separation are simulated. Largest response is expected at a separation of $8 \mu\text{m}$.

the bolometer volume [9]

$$P_{\text{ohmic}} = \frac{1}{2} \text{Re} \left\{ \int_{\text{vol}} \vec{E} \cdot \vec{J}^* dv \right\}. \quad (1)$$

The optimum length of the dipole is determined by simulating a single dipole, which is illuminated by a plane wave from normal incidence. Its length is varied and the response is computed. As shown in Fig. 1(a), the predicted bolometer response is largest at a dipole length of $3.2 \mu\text{m}$. The optimum spacing between array elements is determined in a similar fashion. Two dipoles are illuminated from broadside and the power dissipated in the gold of both antennas is computed as a function of their separation. Fig. 1(b) indicates that the largest response of two $3.2\text{-}\mu\text{m}$ -long dipoles is expected for a separation of $8 \mu\text{m}$. The same separation is used for the three- and four-element arrays, although simulations suggest that slight adjustments in the separation may be preferred (8.5 and $8.75 \mu\text{m}$, respectively).

The radiation patterns of the dipole arrays are simulated by varying the angle of incidence of the illuminating plane wave. For each angle, the power dissipated in the array elements is computed. Since the simulated response is proportional to the measured response, the simulated patterns are normalized at broadside before they are compared to the measured ones.

III. ANTENNA RESPONSE MEASUREMENT WITHOUT LEAD-LINE CONTRIBUTIONS

The simulations omit the lead lines for the biasing and read-out circuit, which are necessary to measure the response of the fabricated devices. This circuit is created during the same fabrication step as the antennas. The lead lines are perpendicular to the dipole antenna and are also perpendicular to the polarization of the incident radiation. Similar to the dipole antennas, these gold lead lines respond bolometrically to the incident radiation and contribute a small, but undesirable component to the antenna response.

Our approach is to include a second device on the same substrate as the dipole arrays. This additional device is similar to the array device, but without the dipoles. The measured response from this device is equivalent to the response contribution of the lead lines to the antenna response in the dipole array device. To

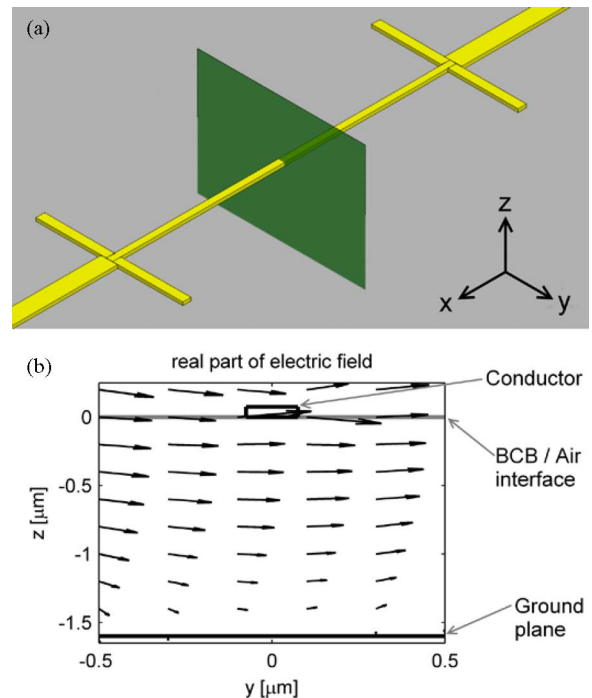


Fig. 2. (a) Layout of a two-dipole array. Highlighted plane at the center of the two dipoles is where the simulated electric field is plotted in (b). The field lines are not pointed between the ground plane and conductor, prohibiting the excitation of a microstrip mode.

ensure the same irradiance on both devices, they are placed in close proximity ($4 \mu\text{m}$) of each other. Simulations indicate that the addition of the second device at the specified distance does not alter the radiation pattern of the antenna array.

In the simulation, the shape of the radiation pattern is created by mutual coupling of the isolated elements in the array. The incident radiation causes a current to flow in each array element, which reradiates parts of the incident wave toward the other array elements. The amount of radiation received by each array element is the vector sum of the incident wave and the reradiated waves from the surrounding array elements [10]. The lead lines, which are omitted in the simulation, connect the dipoles with a narrow strip at the center of the antenna. A microstrip waveguide configuration is formed, since the lead lines are located above a ground plane. However, the microstrip serves only as a signal extraction interconnect rather than as a waveguide, since the contact with the dipole is not designed to couple a propagating waveguide mode. If the device geometry does not support a propagating mode in this waveguide, no additional coupling between the array elements will occur and the aforementioned modeling approach is valid.

The incident radiation illuminating the dipoles is cross polarized to any mode that could propagate along the microstrip. It is therefore unlikely that a microstrip mode will be excited and, as a validation, a two-dipole array including a section of the lead lines is simulated. The layout is shown in Fig. 2(a). The yz -plane located at the center of the two dipoles is highlighted, and the real part of the electric field in this plane is shown in Fig. 2(b). The array is illuminated by a plane wave, polarized along the

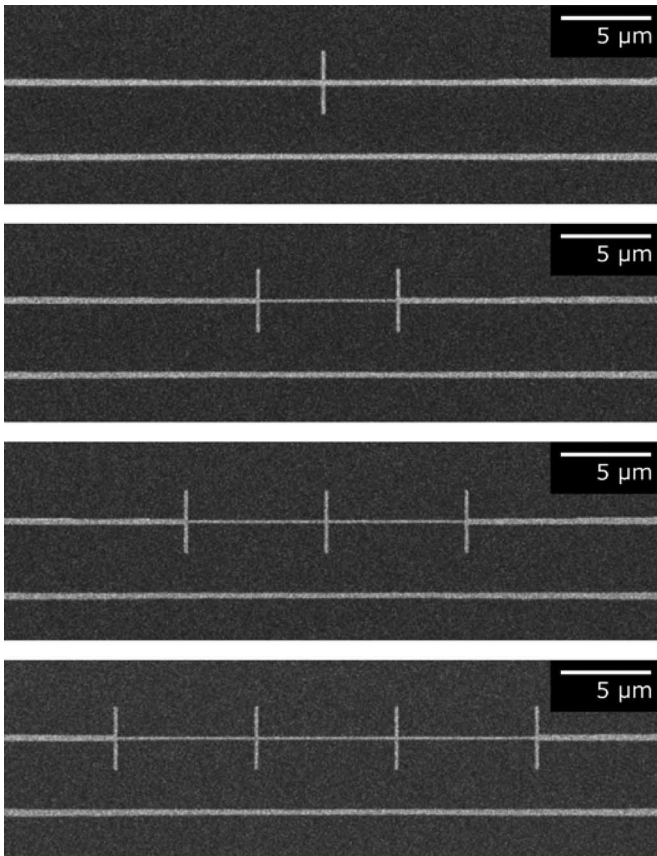


Fig. 3. Scanning electron micrographs of one-, two-, three-, and four-dipole array. The additional devices that measure the lead-line response contributions are adjacent to the antenna arrays.

y -axis, and propagating along the z -axis. The field lines are not oriented between the ground plane and the conducting strip, as expected for a microstrip mode, but instead are parallel to the incident radiation. Therefore, the lead lines do not add to the coupling between the dipole elements and the response of the array elements can be determined by subtracting the measured lead-line contribution from the measured array response.

IV. DEVICE FABRICATION

To form the ground plane, a low-resistivity silicon wafer is coated with 80 nm of thermally evaporated aluminum. It functions as a reflector at 28.3 THz, since its thickness is of multiple skin depths [4]. A 1.6- μm thick layer of BCB is spun onto the wafer and is coated with 400 nm of ZEP 520 A-7. The antenna pattern is exposed using an electron-beam lithography system (Leica EBPG 5000+) at a dose of 120 $\mu\text{C}/\text{cm}^2$. The beam current is 25 nA, and the spot size is 25 nm. The wafer is developed in xylene (ZEP-RD) for 90 s followed by a 1-min oxygen plasma descum etch. The devices are metalized with 75 nm of electron-beam-evaporated gold. A 5-nm-thick adhesion layer of titanium is used. The excess resist and metal are lifted off in a methylene chloride bath. The final devices are shown in scanning electron micrographs in Fig. 3.

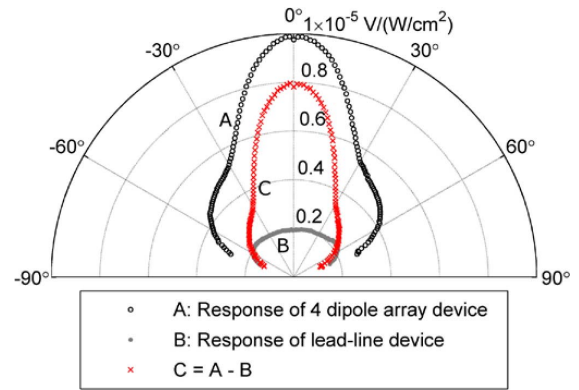


Fig. 4. Measured H -plane radiation pattern of four-dipole array and lead-line contribution. Difference of these two measurements shows the radiation pattern of the four-dipole array without lead-line contributions.

V. RESULTS AND MEASUREMENTS

The device is illuminated using a CO_2 laser operating at 10.6 μm . The power of the laser is reduced using neutral density filters. A $\lambda/2$ waveplate is used to ensure that the polarization is parallel to the dipoles of the antenna arrays. A beam splitter directs a small portion of the laser beam to a reference detector to monitor the fluctuations in the laser power. The reference detector was calibrated to show the power falling onto the devices. A knife edge test showed that the beam spot is 230 μm . The device is biased at 100 mV, and the output signal is amplified ten times using a low-noise amplifier. This signal is then connected to a lock-in amplifier, which is referenced to the 2.5 kHz frequency of a chopper modulating the laser.

The device is mounted onto a five-axis goniometer and aligned, so that the axis of rotation of the goniometer is in the same location as the device and the focus of the laser. The goniometer scans the H -plane from -70° to $+70^\circ$, stopping every 1° to record a measurement. The measured signal, reference power, and angular location of the device are captured using a computer that controls the position of the goniometer.

The measured response V_{out} (in volts) is normalized to the irradiance of the incident laser beam E_{in} (in watt per square centimeter), i.e., $\mathfrak{R}_{\text{out}} = V_{\text{out}}/E_{\text{in}}$. This removes any fluctuations in the response caused by fluctuations in the laser power. The normalization is possible, since an uncooled metal bolometer has a constant TCR [11], and therefore, its response depends linearly on a change in temperature caused by the incident irradiance.

The measured response of a four-element dipole array along with the measured lead-line response is shown in Fig. 4. Since the measured response for the array is a superposition of the distributed-antenna response and lead-line response, the antenna response can be found by subtracting the measurements from each other. The measured antenna response without lead-line contributions is also shown.

Instead of measuring the two devices individually and subtracting the results, the devices can be biased simultaneously and connected to the difference input of the lock-in amplifier similar to the experiment shown in [12]. This shortens the measurement

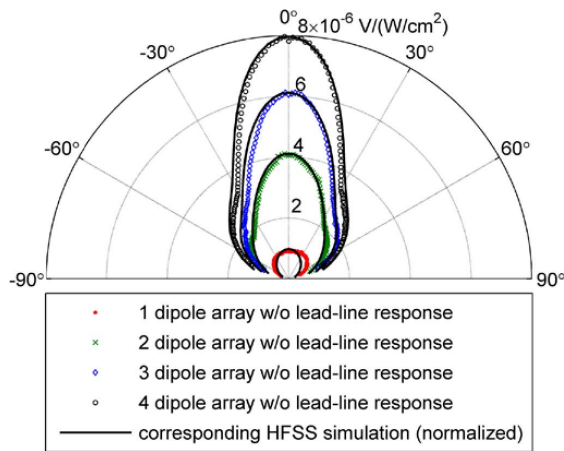


Fig. 5. Measured antenna response without lead-line contributions of one-, two-, three-, and four-dipole arrays. The corresponding simulated radiation patterns are normalized to the broadside response of each measured pattern.

process since the radiation pattern of the antenna response without the lead-line contributions is measured directly.

The radiation pattern of the remaining one-, two-, and three-dipole arrays were measured, and the measured lead-line contribution to each antenna array was subtracted. The result for all four arrays is shown in Fig. 5. The measured radiation pattern is compared to the corresponding simulation results, which are normalized to the appropriate measured radiation pattern at broadside. The shape of the measured and simulated patterns shows excellent agreement.

VI. CONCLUSION

The concept of a distributed bolometric antenna has been introduced. Unlike an antenna-coupled bolometer, where the antenna is used to couple energy into a discrete bolometric element, the entire antenna is composed of the same bolometric material. The simulation process for a receiving antenna using Ansoft HFSS has been described.

The fabricated antenna is only useful if a biasing and read-out circuit is included. This circuit also responds to the incident radiation. A reference device placed in close proximity to the antenna can be used to measure this contribution. Independence of the antenna and lead-line response has been shown, and the response of the antenna elements alone has been measured by subtracting the measured lead-line contribution from the measured response of the antenna device, which includes the lead-line response. Measured radiation patterns of one-, two-, three-, and four-element arrays show excellent agreement with the shape of the simulated patterns. This shows that the simulation process can be used to optimize a particular antenna design.

REFERENCES

- [1] E. N. Grossman, J. E. Sauvageau, and D. G. McDonald, "Lithographic spiral antennas at short wavelengths," *Appl. Phys. Lett.*, vol. 59, no. 25, pp. 3225–3227, Dec. 1991.
- [2] F. J. Gonzalez, B. Ilic, J. Alda, and G. D. Boreman, "Antenna-coupled infrared detectors for imaging applications," *IEEE J. Sel. Topics Quantum Electron.*, vol. 11, no. 1, pp. 117–120, Jan.–Feb. 2005.

- [3] D. R. Lide, *CRC Handbook of Chemistry and Physics*, 84 ed. Boca Raton, FL: CRC Press, 2003.
- [4] J. Ginn, D. Shelton, P. Krenz, B. Lail, and G. Boreman, "Altering infrared metamaterial performance through metal resonance damping," *J. Appl. Phys.*, vol. 105, no. 7, pp. 074304-1–074304-8, Apr. 2009.
- [5] H. F. Hofmann, T. Kosako, and Y. Kadoya, "Design parameters for a nano-optical Yagi-Uda antenna," *New J. Phys.*, vol. 9, no. 7, p. 217, 2007.
- [6] M. E. Mills, P. Townsend, D. Castillo, S. Martin, and A. Achen, "Benzocyclobutene (DVS-BCB) polymer as an interlayer dielectric (ILD) material," *Microelectron. Eng.*, vol. 33, no. 1–4, pp. 327–334, Jan. 1997.
- [7] J. Ginn, B. Lail, D. Shelton, J. Tharp, W. Folks, and G. Boreman, "Characterizing infrared frequency selective surfaces on dispersive media," *ACES J.*, vol. 22, no. 1, pp. 184–188, Mar. 2007.
- [8] P. L. Richards, "Bolometers for infrared and millimeter waves," *J. Appl. Phys.*, vol. 76, no. 1, pp. 1–24, Jul. 1994.
- [9] J. D. Jackson, *Classical Electrodynamics*, 3rd ed. New York: Wiley, 1999.
- [10] C. A. Balanis, *Antenna Theory: Analysis and Design*, 2nd ed. New York: Wiley, 1997, pp. 422–425.
- [11] A. Tanaka, S. Matsumoto, N. Tsukamoto, S. Itoh, K. Chiba, T. Endoh, A. Nakazato, K. Okuyama, Y. Kumazawa, M. Hijikawa, H. Gotoh, T. Tanaka, and N. Teranishi, "Infrared focal plane array incorporating silicon IC process compatible bolometer," *IEEE Trans. Electron Devices*, vol. 43, no. 11, pp. 1844–1850, Nov. 1996.
- [12] P. Krenz, J. Alda, and G. Boreman, "Orthogonal infrared dipole antenna," *Infrared Phys. Technol.*, vol. 51, no. 4, pp. 340–343, Mar. 2008.



Peter M. Krenz (S'04) received the B.S. degree in electrical engineering from Oklahoma State University, Stillwater, in 2003, and the M.S. degree in optics from the University of Central Florida, Orlando, in 2008, where he is currently working toward the Ph.D. degree in optics from the College of Optics and Photonics (CREOL).

He is currently a Graduate Research Assistant at the College of Optics and Photonics (CREOL). His research interests include the simulation, fabrication, and characterization of uncooled antenna-coupled infrared detectors.



Brian A. Lail received the B.S. degree in physics from Furman University, Greenville, SC, and the M.S. degree in physics and electrical engineering and the Ph.D. degree in electrical engineering from New Mexico State University, Albuquerque.

From 2002 to 2005, he was in the Department of Electrical and Computer Engineering, University of Central Florida, Orlando. Since 2005, he has been an Assistant Professor in the Department of Electrical and Computer Engineering, Florida Institute of Technology, Melbourne, where he has been engaged in teaching and conducting research in applied and computational electromagnetics.



Glenn D. Boreman received the B.S. degree in optics from the University of Rochester, Rochester, NY, and the Ph.D. degree in optics from the University of Arizona, Tucson.

He has been a Visiting Scholar at Imperial College, London, Swiss Federal Institute of Technology (ETH), Zürich, Complutense University, Madrid, University of New Mexico, Albuquerque, and Swedish Defense Research Agency (FOI), Linköping, Sweden. He is currently a Trustee Chair Professor of optics at the College of Optics and Photonics (CREOL), University of Central Florida, Orlando. For six years, he was an Editor-in-Chief of the *Applied Optics*. He is currently an Associate Editor of the *Optics Express* and is also an Editor of the *Wiley Series in Pure & Applied Optics*. He is the coauthor of the *Infrared Detectors and Systems*, and the author of the *Modulation Transfer Function in Optical and Electro-Optical Systems*, and the *Basic Electro-Optics for Electrical Engineers*.

Prof. Boreman is a Fellow of the Military Sensing Symposium, the Optical Society of America, and the International Society for Optical Engineering.